Study of the correlated walks with reflecting walls[a)]

Y. Okamura[b)] and E. Blaisten-Barojas

Instituto de Fisica, Universidad Nacional Autónoma de México, AP 20-364, México 20, D.F., México

S. V. Godoy and S. E. Ulloa[c)]

Facultad de Ciencias, Universidad Autónoma de México, México 20, D. F.,México

S. Fujita[c)]

Theoretical Physics Institute, University of Alberta, Edmonton, Alberta, Canada T6G 2J1
and Instituto de Fisica, Universidad Nacional Autónoma de México, México 20, D. F.,México
(Received 26 January 1981; accepted 6 February 1981)

Exact expressions for the arrival probabilities with direction are obtained for correlated walks on an infinite line. The probability distribution exhibits a diffusive maximum, similar to that characteristic of random walks, *and a runaway component* which is associated with free passage (no scattering). For symmetric step probabilities, the arrival probabilities for a finite line bounded by reflecting walls are expressible in terms of free-space probabilities. The evolution of the system of probabilities is studied in terms of the Boltzmann H function. The system approaches equilibrium monotonically. In general, there exists an optimum degree of correlation between successive steps at which the randomization in space and direction proceeds most rapidly. At lower correlation the system moves like a wave packet with dissipation. The randomization in space is aided by the reflecting walls (and by the periodic boundary).

I. INTRODUCTION

In the correlated walks in one dimension an object moves right or left with probabilities which, by assumption, depend on the direction of the last step. This model was introduced by Goldstein and others[1] as a generalization of the random walks, which have been studied quite extensively.[2] On the basis of the correlated walk model we recently discussed the conformation of a simple polymer,[3] the atomic diffusion in crystals with defects,[4] and the nonequilibrium properties of a Lorentz gas.[5] The Ising problem can also be treated in terms of this model and its generalizations.[6]

The dynamics of correlated walks is quite different from that of random walks when the directional correlation is strong. In particular, we demonstrated in Ref. 6 that the fluctuations can be extremely large near the high correlation limit. In such a case, the behavior of the walker cannot be described adequately in terms of a few moments such as averages of displacement $\langle x \rangle$ and squared displacements $\langle x^2 \rangle$. It is found possible to obtain an explicit expression for the probability distribution in the one-dimensional correlated walks, which constitutes one of the purposes of the present work. It will be shown that in the high correlation region the distribution can have two maxima, a diffusive maximum similar to that of the Bernoulli distribution *and* a *runaway component* which is associated with free passage and which strongly depends on the initial condition. When this component is present, the dynamics cannot be described in terms of a finite number of moments.

In many physics problems, the boundary plays important roles. In the present paper we take up the reflecting wall and the periodic boundary, both of which limit the walker's range. It will be shown that the arrival probabilities for either case can be expressed in terms of free-space probabilities for the symmetric correlated walks. Using these results, we discuss the evolution of the probabilities to equilibrium. The approach to equilibrium, which is studied by means of the Boltzmann H function, shows distinct behaviors, depending on the type of boundary and the separation of reflecting walls.

In the present work, calculations are carried out on the one-dimensional walks. When appropriate, however, we will point out the general results applicable to higher dimensions.

In Sec. II we present the basic recurrence equations, and their solutions, for the correlated walks in one dimension. The derivation of the arrival probabilities with direction is sketched in the Appendix. The runaway component, which appears in the high correlation region, is demonstrated and discussed in Sec. III. Correlated walks with reflecting walls and with a periodic boundary condition are defined and solved in Sec. IV. In Sec. V we discuss the evolution of the probabilities to equilibrium. A brief summary is given in Sec. VI.

II. CORRELATED WALKS

Let us consider a linear lattice of infinite extension. An object will move along the line right or left with given jump probabilities, which depend on the direction of the previous step. Let us say that the right and left steps are steps of type 1 and 2, respectively. If the last step is of type j, the probabilities of stepping right and left will be denoted by p_j and q_j with the normalization

$$p_j + q_j = 1 , \quad j = 1, 2 . \tag{2.1}$$

[a)]Work supported in part by CONACYT, Mexico, project PNCB-0024.

[b)]Present address: Department of Chemistry, McGill University, Montreal, P. Q., Canada H3A 2K6.

[c)]Present address: Department of Physics and Astronomy, State University of New York at Buffalo, Amherst, N. Y., 14260.

 0021-9606/82/010601-08$02.10

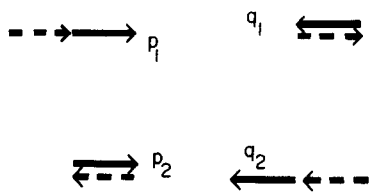

FIG. 1. The step probabilities, which by assumption depend on the previous step, are designated by (p_1, q_1, p_2, q_2).

The definitions of the step probabilities are schematically shown in Fig. 1.

Let $W_j(x, N)$ be the probability that the walker arrives at the position x with the steptype j after N steps. The W_j satisfy

$$W_1(x,N)=p_1W_1(x-1,N-1)+p_2W_2(x-1,N-1)\,, \quad (2.2)$$

$$W_2(x,N)=q_1W_1(x+1,N-1)+q_2W_2(x+1,N-1)\,. \quad (2.2a)$$

These equations can be obtained by considering the dynamics of two successive steps. For definiteness, let us assume that the walker arrived at x_0 with the step type 1 at the initial time $N=0$. The solution of Eqs. (2.2) with this initial condition can be obtained with the aid of the auxiliary-lattice-and-generating-function techniques,[6] and will be denoted by $W_j(x, N; x_0)$. Since the dynamics is the same all along the line, we can deduce that

$$W_j(x,N;x_0)=W_j(x-x_0,N;0)\equiv w_j(x-x_0,N)\,, \quad (2.3)$$

where a new function w_j is introduced. This equation expresses a simple translation property that the solution with an arbitrary starting point x_0 can be obtained in terms of the solution with the starting point 0. Explicit expressions for w_j, whose derivation is sketched in the Appendix, are as follows:

$$w_j(x,N)=\begin{cases} Q_j[\tfrac{1}{2}(N+x),N]\,, & \text{if } N+x \text{ is even and nonnegative}\,,\\ 0\,, & \text{otherwise}\,, \end{cases} \quad (2.4)$$

where

$$Q_1(X,N)=\begin{cases}\delta_{N,0}\,, & X=0\\ \displaystyle\sum_{r=0}^{X}\binom{N-r-1}{X-1}\binom{X}{r}p_1^{X-r}q_2^{N-X-r}(p_2q_1-p_1q_2)^r\,, & 1\le X\le N\,,\\ 0\,, & X=N\end{cases}$$

$$Q_2(X,N)=\begin{cases}\displaystyle\sum_{r=0}^{X}\binom{N-r-1}{X}\binom{X}{r}p_1^{X-r}q_1q_2^{N-X-r-1}(p_2q_1-p_1q_2)^r\,, & 0\le X<N\,.\end{cases} \quad (2.5)$$

III. PROBABILITY DISTRIBUTION: RUNAWAY COMPONENT

The arrival probabilities, given in Eqs. (2.4) and (2.5), depend on p_1, p_2, q_1, q_2, and N in a complicated manner. From now on, we will consider a less general situation. Let us assume the *right–left symmetry* on the step probabilities such that

$$p_1=q_2\equiv\alpha\,, \quad p_2=q_1\equiv\beta\,, \quad \alpha+\beta=1\,. \quad (3.1)$$

The probability of making a step in the same direction as that of the previous step is denoted by α, and the probability of making a reversing step by β.

In our earlier work,[6] we calculated the mean and mean square displacements $\langle x\rangle_N$ and $\langle x^2\rangle_N$, respectively, as a function of time N. It was found that if the *degree of correlation* defined by

$$\delta\equiv\alpha-\beta \quad (3.2)$$

is small, these averages are similar to those corresponding to the usual random walks

$$\langle x\rangle_{\text{random}}=0\,, \quad \langle x^2\rangle_{\text{random}}=N\,. \quad (3.3)$$

However, if δ is close to unity, the results are quite different, and large fluctuations occur. In fact, the limit behavior is as follows:

$$\langle x\rangle_N\to N\,, \qquad \langle x^2\rangle_N\to N^2\,, \quad \text{as } \delta\to 1\,. \quad (3.4)$$

When large fluctuations exist, it is not appropriate to discuss the dynamics of the walker in terms of the first and second moments, $\langle x\rangle$ and $\langle x^2\rangle$, alone. A better way of looking at the dynamics is to study the arrival probabilities directly.

The probability of the object arriving at (x, N) from any any direction $w(x, N)$ is given by

$$w(x,N)\equiv w_1(x,N)+w_2(x,N)\,. \quad (3.5)$$

The w_j can be obtained in terms of Q_j [see Eq. (2.4)]. After introduction of Eq. (3.1) in Eq. (2.5), we obtain

$$Q_1(X,N)=\begin{cases}\displaystyle\sum_{r=0}^{X}\binom{N-r-1}{X-1}\binom{X}{r}\alpha^N\left(\frac{\beta-\alpha}{\alpha^2}\right)^r, & 1\le X\le N\,,\\ \delta_{N,0}\,, & X=0\,,\end{cases}$$

$$Q_2(X,N)=\begin{cases}\displaystyle\sum_{r=0}^{X}\binom{N-r-1}{X}\binom{X}{r}\beta\alpha^{N-1}\left(\frac{\beta-\alpha}{\alpha^2}\right)^r\,, & 0\le X<N\,,\\ 0\,, & X=N\,.\end{cases} \quad (3.6)$$

In Fig. 2 we show how this probability distribution w behaves for different values of the parameter α. The case of $\alpha=\beta=0.5$ corresponds to that of random walks, where the distribution is symmetric about the starting point 0. For the values of α close to unity, there arise a diffusive maximum, similar to that associated with random walks, *and a runaway component* which is associated with free passage (no scattering) and which strong-

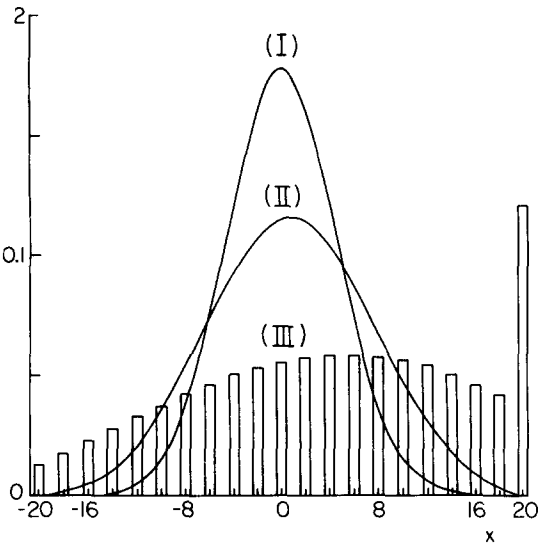

FIG. 2. The arrival probability distribution $w(x, N)$ for $x \equiv m - m_0$, $m_0 = 0$, $N = 20$, and different α values: (I) $\alpha = 0.5$, (II) $\alpha = 0.7$, and (III) $\alpha = 0.9$. The case (III), represented by a histogram, exhibits the runaway component at $x = 20$. Other cases are indicated by continuous curves rather than histograms.

ly depends on the initial condition (see the histogram for $\alpha = 0.9$). This component numerically equals α^N. In between these two extremes, the diffusive maximum becomes flattened faster as α grows from 0.5 to unity.

The runaway component which appears when α is close to unity is a most significant feature of the correlated walks, distinct from the random and Bernoulli walks whose distributions are characterized by single maxima. As stated earlier, when this component is present, the fluctuations can be very large.

IV. CORRELATED WALKS WITH REFLECTING WALLS

For the sake of convenience, let us displace the origin 0 by half a lattice spacing so that all the sites have half-integers as coordinates, as indicated in Fig. 3.

Let us now put a reflecting wall at the origin. The object which by assumption started at a positive site x_0 initially can move only on the positive side of the lattice. The reflecting wall dictates that every time the object hits the wall, it will change the direction of its motion, and return to the position $x = \frac{1}{2}$. In mathematical terms, we may express this as follows:

$$W_1(\tfrac{1}{2}, N) = \beta W_1(\tfrac{1}{2}, N-1) + \alpha W_2(\tfrac{1}{2}, N-1) . \qquad (4.1)$$

In addition, Eq. (2.2) is valid for $x \geq \frac{3}{2}$ and Eq. (2.2a) for $x \geq \frac{1}{2}$.

For small N, we can follow the possible motion of the walker by drawing paths in the x–N diagram as shown in Fig. 4, the case in which $x_0 = \frac{3}{2}$ and $N = 0, 1, 2, 3, 4$. The probabilities of arrival at points (x, N), i.e., $W_1(x, N)$ and $W_2(x, N)$, can be obtained simply from the diagram, and are given explicitly. For comparison, the dynamics of the walker for a free space with the same initial condition is shown in Fig. 4(b).

A good deal of similarity exists between the two. If we reflect the negative part of Fig. 4(b) with respect to the line at $x = 0$, we get the same figure as Fig. 4(a). In particular, corresponding to any given path in Fig. 4(a), we can find the path in Fig. 4(b) by means of the reflection. The corresponding pair of paths carry the *same* factors of step probabilities. We further observe that if a path in Fig. 4(a) does not hit the wall or hits an even number of times, the corresponding path in Fig. 4(b) ends at the *same site* with the *same direction*. If a path in Fig. 4(a) hits the wall an odd number of times and terminates at the site (x, N), the corresponding path in Fig. 4(b) ends at the site $(-x, N)$ with the *opposite direction*. The probabilities of arrival $W_j(x, N; x_0)$ are obtained by summing over all possible paths. We may then infer that these probabilities W_j for a semibounded space are expressed in terms of the corresponding free-space probabilities $W_j^{(f)}$ as follows:

$$W_j(x, N; x_0) = W_j^{(f)}(x, N; x_0) + W_{j^*}^{(f)}(-x, N; x_0) , \qquad (4.2)$$

where j^* denote the conjugates of j, i.e.,

$$(1^*, 2^*) \equiv (2, 1) . \qquad (4.3)$$

Equation (4.2) was obtained from the special case of $x_0 = \frac{3}{2}$ and $N = 0, 1, 2, 3, 4$. However, it holds in general. We note that the free-space probabilities $W_j^{(f)}$ can be obtained from Eqs. (2.3), (2.4), and (3.6).

Let us now put another reflecting wall at $x = L$, with L being a positive integer. There will be L lattice points between the two walls. The motion of the walker is then restricted to the domain $\frac{1}{2}, \frac{3}{2}, \ldots, (2L-1)/2$.

By extending the mirror-image techniques, it is possible to show that the arrival probabilities $W_j(x, N; x_0)$ can be expressed in terms of the free-space probabilities as follows:

$$W_j(x, N; x_0) = \sum_{k=-\infty}^{\infty} [W_j^{(f)}(2kL + x, N; x_0) + W_{j^*}^{(f)}(2kL - x, N; x_0)] , \qquad (4.4)$$

where k runs over integers.

For the sake of comparison, let us consider the periodic boundary condition, which may be set up by form-

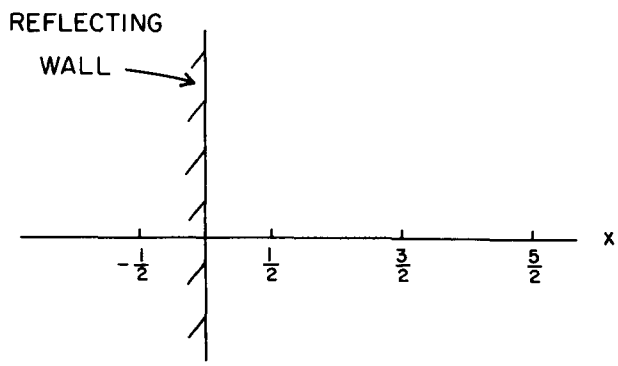

FIG. 3. The sites are numbered by half-integers. A reflecting wall is placed at the origin. The object which started at a positive site can now move on the positive side only.

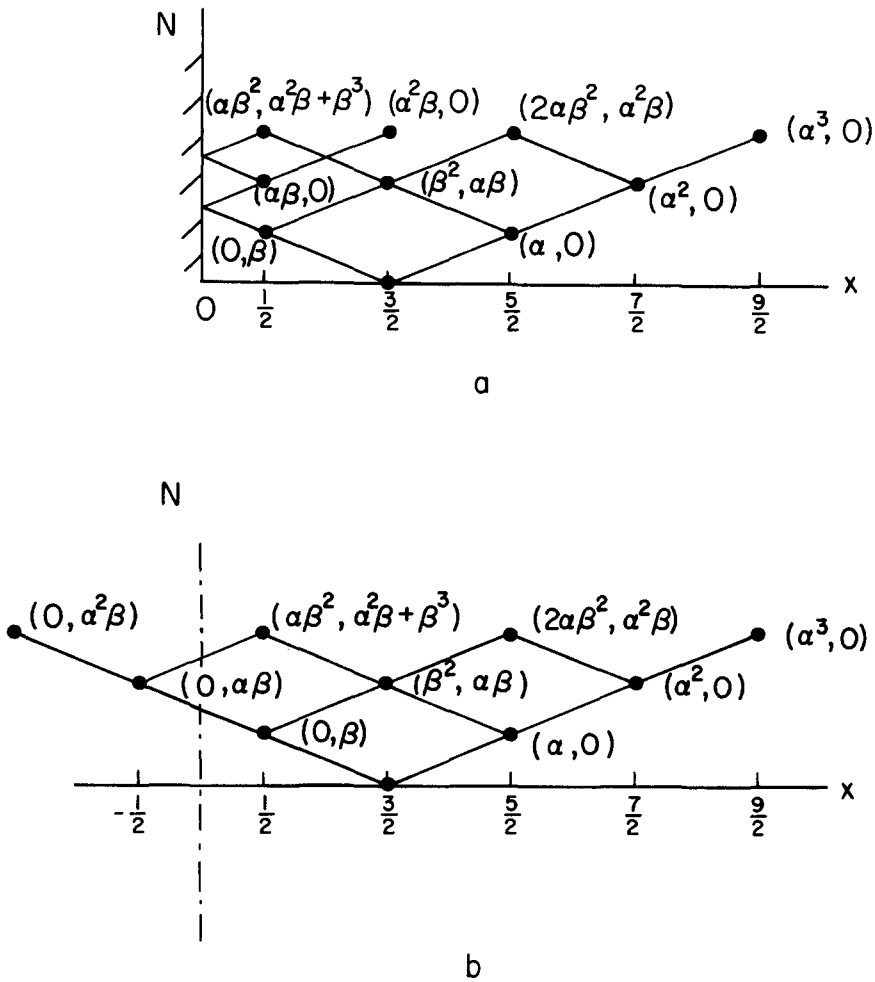

FIG. 4. The possible paths of the walker who arrived at $x_0 = 3/2$ from the left with and without the reflecting wall at the origin are shown in (a) and (b), respectively. The arrival probabilities with direction $[W_1(x,N;\ x_0 = 3/2),\ W_2(X,N;\ x_0 = 3.2)]$ are given at all sites for $N = 1$, 2, and 3.

ing a loop of length L. The object may now move with the same rule everywhere along the loop.

The arrival probabilities $W_j(x, N; x_0)$ for this boundary can be expressed as follows:

$$W_j(x, N; x_0) = \sum_{k=-\infty}^{\infty} W_j^{(f)}(kL + x, N; x_0) . \tag{4.5}$$

This result may be obtained in a much simpler manner than the corresponding result (4.4) for the reflecting boundary.

We derived our main results [Eqs. (4.2) and (4.4)] with the assumption that the lattice points are denoted by half-integers in units of the lattice constant. Since the probabilities $W_j^{(f)}$ have the translation-invariant property (2.3), we may lift the above assumption altogether in the final results (4.2), (4.4), and (4.5). In other words, if desired, we may designate all the sites by integers and the positions of walls by half-integers.

V. THE *H* FUNCTION: THE APPROACH TO EQUILIBRIUM

In our model the object will always move with the same speed. Irrespective of how the walker started initially, it will eventually arrive from either direction at any and every allowed lattice point with the same probability (unless $\alpha = 1$). In order to study the approach to this stationary state, let us introduce the Boltzmann H function defined by

$$H(N) = \sum_{j=1}^{2} \sum_{x} W_j(x, N; x_0) \ln W_j(x, N; x_0) , \tag{5.1}$$

where the variable x runs between the two walls. This function $H(N)$, calculated from Eq. (4.4) for the case of $L = 8$ and $x_0 = 2$, is shown in solid lines in Fig. 5. Unless $\alpha = 1$, i.e., if we allow scatterings to occur, our system approaches a stationary state in a *monotonic* manner. The stationary state corresponds to the state in which all "particle" states with the same energy are occupied with the same probability, as characterized by the microcanonical ensemble. The entropy of the system will be defined by

$$S(N) = -k_B H(N) , \tag{5.2}$$

where k_B is the Boltzmann constant.

This entropy is at maximum in the stationary state, and is given by

$$S(\infty) = k_B \ln(2L) . \tag{5.3}$$

The manner in which it approaches equilibrium depends on the step probabilities (α, β) and the separation of the walls in a rather complicated manner. To understand this behavior we consider the following two limiting cases.

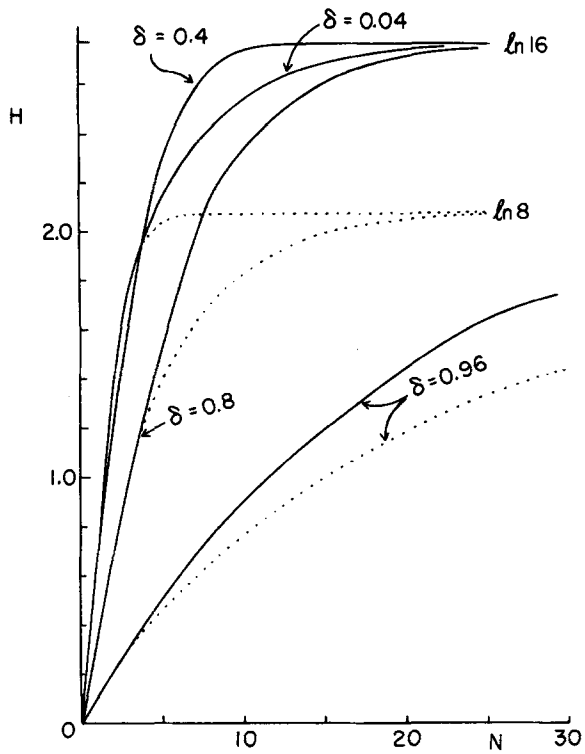

FIG. 5. The negative of the H function (5.1) with $x_0 = 2$ and $L = 8$ against the time N is shown for different values of δ. The solid lines correspond to the reflecting walls and the dotted lines to the periodic boundary condition.

A. The extreme case of small separation: $L = 1$

The extreme case of small separation is that of a single site: $L = 1$. Such a case in three dimensions was studied in detail and reported in Ref. 5. The randomization in direction for this case is of an exponential-decay type characterized by the relaxation time

$$\tau_R = \frac{1+\delta}{1-\delta}\tau_0 , \tag{5.4}$$

where τ_0 is the unit time in which the object moves from one site to next.

The system approaches equilibrium more slowly as the degree of correlation δ is raised from 0 (random walks) to unity (no scattering). This behavior can be seen from Eq. (5.4), which indicates a greater relaxation time for higher δ.

B. The extreme case of large separation: $L = \infty$

The extreme case of large separation is that of free space. The H function, calculated from Eq. (5.1) with $W_j = W_j^{(f)}$, decreases indefinitely since the accessible sites are infinitely many. The behavior of the negative of $H(N)$ against the degree of correlation δ is shown in Fig. 6. Each curve for $N > 2$ has a single maximum at $\delta = \delta_m$.

The appearance of the maximum may be understood as follows: When the correlation is negligible ($\delta \cong 0$), the arrival probabilities for small N are localized near the starting point x_0 and nearly at random in direction. Subsequently, this cloud of probabilities will spread out. This spreading out, i.e., the randomization in space, is a diffusion process, which is characterized by the diffusion coefficient

$$D = v^2\tau_R = v^2\frac{1+\delta}{1-\delta}\tau_0 . \tag{5.5}$$

where $v \equiv a_0/\tau_0$ is the speed of the walker. Since the value of D is greater for larger δ, the randomization in space proceeds *faster* as the degree of correlation δ is raised from 0. This explains the initial positive slope near $\delta = 0$ in Fig. 6. If, however, the correlation is so large that $\delta \cong 1$, then the arrival probabilities should hardly spread out and the H function must remain small in magnitude. In summary, the negative of the H function should increase near $\delta = 0$ and, after passing through a maximum, should go to zero at $\delta = 1$.

The position of the maximum δ_m grows with the time $N\tau_0$. This behavior is shown in Fig. 7. The monotonic curve divides the δ–N plane in two regions, a diffusion-dominated region characterized by small δ and a high-correlation region characterized by high δ. The second region, it is noted, is the region where the runaway component discussed in Sec. III may play a significant role.

Let us now go back to Fig. 5, the case of the reflecting walls with the separation length $L = 8$ and the starting point $x_0 = 2$. At $N = 2$, the negative of the H function has higher values for smaller δ. This pattern is reversed for the cases of $\delta = 0.04$ and 0.4 for $N \geqq 4$, i.e., for a moderate degree of correlation ($\delta = 0.4$) the system approaches the stationary state faster than for the zero correlation (random walks $\delta = 0$). The H func-

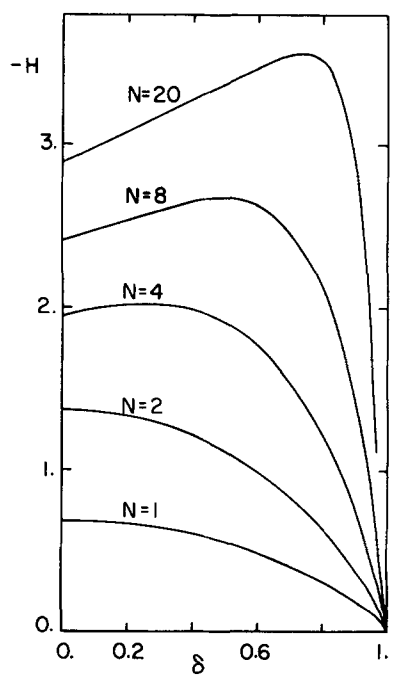

FIG. 6. The negative of the H function (5.1) for free space ($L = \infty$) against the degree of correlation δ is plotted for different values of the time N.

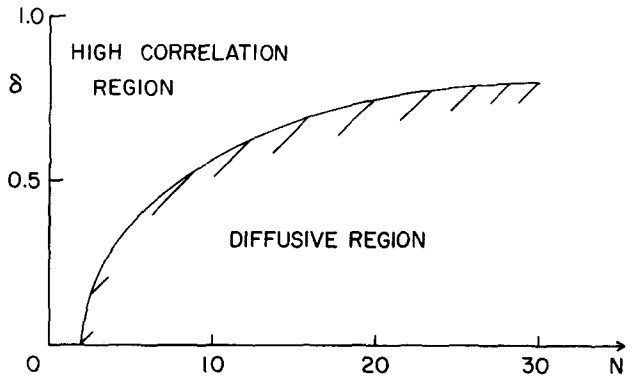

FIG. 7. The optimum degree of correlation at which the randomization in space and direction proceeds most rapidly, depends on the time N and the separation length L. The case of free space ($L=\infty$) is shown here. The curve separates the diffusion-dominated region from the high correlation region in a general manner.

tion approaches equilibrium in almost every case at $N=20$ except for δ higher than 0.8. This is so due to the reflecting walls. In Fig. 8 we show $-H$ vs δ at $N=20$ for different boundaries—reflecting walls, free space, and periodic boundary.

In many physics calculations, the periodic boundary condition is used for mathematical convenience. When the boundary plays little or no role, this is an acceptable substitute for a more realsitic boundary such as reflecting walls. The approach to equilibrium in general depends on the boundary condition. The H functions calculated on the basis of the solutions (4.5) are indicated by dotted lines in Figs. 5 and 8. A significant feature for this boundary is that for even L the entropy $S(N)\equiv -k_B H(N)$ approaches $k_B \ln(L)$ while the entropy for odd L approaches $k_B \ln(2L)$, which is equal to the stationary value for the system with reflecting walls. This difference may be understood in the following manner: In free space, the object starts at some point x_0 and must move either right or left [see Fig. 4(b)]. After N units of time it arrives at sites x which satisfy the condition that $N+x-x_0$ be even and nonnegative. Because of this restriction on the motion, the object cannot cover all sites uniformly. When the periodicity length L is even, the restriction is fully in force and the object can reach only half of the total sites at any given time. If L is odd, the restriction is lifted at the boundary. [The restriction is lifted at reflecting walls for any L; see Fig. 4(a).] Then, the system approaches the state of maximum entropy given by Eq. (5.3).

VI. SUMMARY

In the present work, exact expressions (2.4) for the arrival probabilities with direction $W_j(x, N; x_0)$ were obtained for the correlated walks on an unbounded line. A significant feature distinct from the Bernoulli distribution is the existence of the runaway component, whose value equals p_1^N. This component may even be greater in magnitude than the diffusive maximum. This maximum flattens faster for higher values of the degree of correlation $\delta=\alpha-\beta$ and its decay rate is characterized by the diffusion coefficient $D=v^2\tau_R$.

The correlated walks may be subjected to various boundary conditions. In the present work, we considered the reflecting walls and periodic boundary only. For these boundaries we were able to express the arrival probabilities W_j in terms of the free-space probabilities $W_j^{(f)}$ [see Eqs. (4.4) and (4.5)], if the right–left symmetry in step probabilities ($p_1=q_2\equiv\alpha$, $p_2=q_1\equiv\beta$) is assumed. The mirror-image method, which was used to obtain the results for the case of the reflecting walls, breaks down for general asymmetric step probabilities (p_1, q_1, p_2, q_2). The probabilities of eventual absorption at the absorbing walls, which limits the range of the correlated walks, were calculated earlier.[7] However, other important properties of correlated walks with absorbing boundaries have not fully been explored. For example, the eventual absorption A at the wall located at the origin, for semibounded Bernoulli walks ($p_1=p_2\equiv p$, $q_1=q_2\equiv q$), is given by[8]

$$A=\begin{cases}(q/p)^{x_0}, & \text{if } q<\frac{1}{2},\\ 1, & \text{if } q\geq\frac{1}{2}.\end{cases} \tag{6.1}$$

How this striking feature will change with introduction of the directional correlation is an important question.

The system of the arrival probabilities with direction W_j evolves to a stationary state in which all allowed W_j are equal to each other unless $\alpha=1$. We studied the approach to equilibrium in terms of the Boltzmann H function. This approach critically depends on the step probabilities, the separation between the walls, and the boundary type. In particular, the following results are obtained:

(a) For small separations, the system reaches equilibrium more slowly as the degree of correlation δ is raised from 0 to unity.

(b) For large separations, the randomization in space proceeds *faster* as δ is raised.

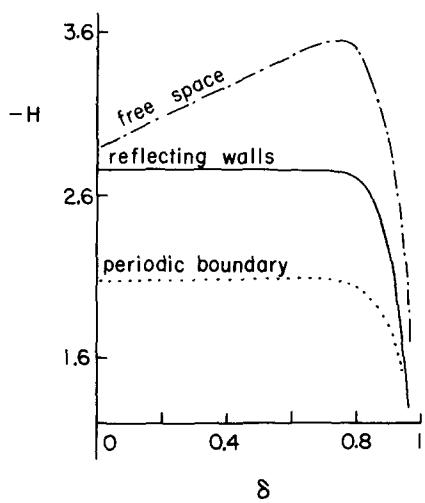

FIG. 8. The negative of the H function (5.1) with $x_0=2$, $L=8$, and $N=20$ against the degree of correlation is shown for three types of boundaries.

(c) The reflecting walls and periodic boundary help e spatial randomization.

(d) There exists *an optimum* δ_m at which the randomization in space and direction proceeds most quickly. or free space, this δ_m is a function of the time $N\tau_0$. $\delta < \delta_m$, the system is diffusion dominated. In the other ase $\delta > \delta_m$, the system moves like a wave packet with issipation.

Our one-dimensional models may be extended for ıigher dimensions. Many qualitative features obtained ıere are expected to hold also for high-dimensional models. In particular, we already know[4,5] that the relaxation time τ_R can be expressed in the form (5.4) independently of the dimensionality and cubic-lattice type.

Finally, the models treated here, if extended for higher dimensions, should be useful for discussions of various phenomena including the sedimentation of particles in solution, atomic diffusions in crystals,[4] polymer conformation statistics,[3] etc.

APPENDIX: DERIVATION OF EQS. (2.4) AND (2.5)

Each step of the correlated walker can be represented in the auxilary square lattice, shown in Fig. 9, provided that the walker's move toward the left is viewed as the upward move on the lattice. In this representation, the object starts at the origin 0 and moves one step right or up per unit time. After N units of time, the object will arrive at a lattice point (X, Y) which satisfies

$$X + Y = N . \tag{A1}$$

Because of this property, we may specify the point of arrival by (X, N). Let the probabilities of the object arriving at the site (X, N) with the right (up) step be $Q_1(X, N)\,[Q_2(x, N)]$. Consideration of two successive steps yields the following relations:

$$\begin{aligned} Q_1(X, N) &= p_1 Q_1(X-1, N-1) \\ &\quad + p_2 Q_2(X-1, N-1) , \quad X > 0, N > 0 , \\ Q_2(X, N) &= q_1 Q_1(X, N-1) \\ &\quad + q_2 Q_2(X, N-1) , \quad X \geqq 0, N > 0 . \end{aligned} \tag{A2}$$

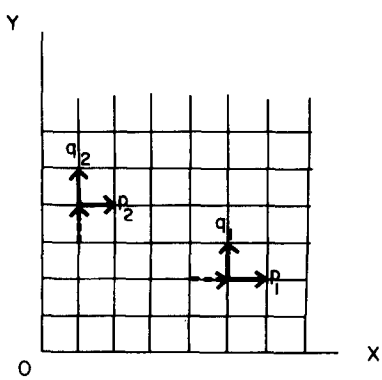

FIG. 9. The step probabilities which depend on the direction of the previous steps for the auxiliary square lattice are given by (p_1, q_1, p_2, q_2) as shown.

These equations correspond to Eqs. (2.2). In fact, the functions Q and W are related by Eq. (2.4). The probabilities Q have nonnegative arguments for both variables X and N. Using this property, we may solve Eqs. (A2) in the following manner:

We assume the initial condition

$$Q_j(X, 0) = \delta_{j,1}\delta_{X,0} , \tag{A3}$$

which corresponds to the fact that the object arrived at the origin with the right step.

Let us introduce generating functions

$$\begin{aligned} \psi_j(\xi, \nu) &\equiv \sum_{N=0}^{\infty} \nu^N \sum_{X=0}^{N} \xi^X Q_j(X, N) , \\ &\equiv \sum_{N=0}^{\infty} \nu^N \sum_{X=0}^{\infty} \xi^X Q_j(X, N) , \\ &\equiv \sum_{x=0}^{\infty} \xi^X \tilde{Q}_j(X, \nu) , \end{aligned} \tag{A4}$$

where the third member was obtained from the second with the aid of the property

$$Q_j(X, N) = 0 , \quad \text{if } X > N . \tag{A5}$$

Multiplying Eqs. (A2) by $\nu^N \xi^X$, summing over (N, X), and using the initial condition (A3), we can get simultaneous equations for ψ_j, whose solutions are as follows:

$$\begin{aligned} \psi_1 &= \frac{1 - \nu q_2}{(1 - \nu q_2)(1 - \nu\xi p_1) - \nu^2 \xi p_2 q_1} , \\ \psi_2 &= \frac{\nu q_1}{(1 - \nu q_2)(1 - \nu\xi p_1) - \nu^2 \xi p_2 q_1} . \end{aligned} \tag{A6}$$

Expanding ψ_1 in powers of ξ as

$$\psi_1 = 1 + \cdots + \left[\frac{p_1\nu - (p_1 q_2 - p_2 q_1)\nu^2}{1 - q_2\nu}\right]^X \xi^X + \cdots$$

and comparing with Eq. (A4), we obtain

$$\begin{aligned} \tilde{Q}_1(X, \nu) &= \frac{[p_1 + (p_2 q_1 - p_1 q_2)\nu]^X \nu^X}{(1 - q_2\nu)^X} \\ &= \sum_{r=0}^{\infty} \binom{X}{r} p_1^{X-r} (p_2 q_1 - p_1 q_2)^r \nu^{X+r} (1 - q_2\nu)^{-X} . \end{aligned} \tag{A7}$$

Applying the formula

$$\frac{1}{(1-y)^X} = \sum_{s=X-1}^{\infty} \frac{s!}{(X-1)!(s-X+1)!} y^{s-X+1} , \quad X \geqq 1 ,$$

we then obtain

$$\begin{aligned} \tilde{Q}_1(X, \nu) = \sum_{r=0}^{X} \sum_{s=X}^{\infty} &\binom{X}{r} p_1^{X-r} (p_2 q_1 - p_1 q_2)^r \\ &\times \frac{s!}{(X-1)!(s-X+1)!} q_2^{s-X+1} \nu^{s+r+1} . \end{aligned} \tag{A8}$$

Comparing this expansion with Eq. (A4), we obtain

$$\begin{aligned} Q_1(X, N) = \sum_{r=0}^{X} &\binom{N-r-1}{X-1} \binom{X}{r} \\ &\times p_1^{X-r} q_2^{N-X-r} (p_2 q_1 - p_1 q_2)^r , \quad 1 \leqq X \leqq N . \end{aligned} \tag{A9}$$

In the case of $X = 0$, we obtain, directly from Eq. (A7),

$$Q_1(0,N)=\delta_{N,0}\ . \tag{A9a}$$

In a similar manner, we may compute $Q_2(X,N)$ from ψ_2 and obtain

$$Q_2(X,N)=\sum_{r=0}^{X}\binom{N-r-1}{X}\binom{X}{r}$$
$$\times p_1^{X-r}q_1q_2^{N-X-r-1}(p_2q_1-p_1q_2)^r\ , \qquad 0\leqq X<N\ .$$

$$Q_2(N,N)=0\ . \tag{A10}$$

The results (A9), (A9a), and (A10) are quoted in Eq. (2.5).

[1]S. Goldstein, Q. J. Mech. Appl. Math. **4**, 129 (1951); G. Klein, Proc. R. Soc. Edinburgh, Sect. A **63**, 268 (1952); J. Gillis, Proc. Cambridge Philos. Soc. **51**, 639 (1955); C. Mohan, Biometrika **42**, 486 (1955); H. C. Gupta, Sankhya **20**, 295 (1958); A. Seth, J. R. Stat. Soc. B **25**, 394 (1963); G. Jain, Can. Math. Bull. **14**, 341 (1971); **16**, 389 (1973); J. R. Manning, *Diffusion Kinetics for Atoms in Crystals* (Van Nostrand, New York, 1968).

[2]S. Chandrasekhar, Rev. Mod. Phys. **15**, 1 (1943); M. C. Wang and G. E. Uhlenbeck, Rev. Mod. Phys. **17**, 90 (1945) W. Feller, *An Introduction to Probability Theory and its Applications* (Wiley, New York, 1957).

[3]S. Fujita, Y. Okamura, and J. T. Chen, J. Chem. Phys. 72 3993 (1980).

[4]Y. Okamura, E. Blaisten-Barojas, S. Fujita, and S. V. Godoy, Phys. Rev. B **22**, 1638 (1980).

[5]S. Fujita, Y. Okamura, E. Blaisten-Barojas, and S. V. God J. Chem. Phys. **73**, 4569 (1980).

[6]S. Fujita and J. T. Chen, Kinam **1**, 177 (1979).

[7]I. Simon and S. Fujita, Acta Phys. Austriaca **50**, 207 (1979).

[8]See Feller's book in Ref. 2, and Y. Okamura, Ph.D. Dissertation, SUNY/Buffalo, 1981.